Analysis and Efficient Solution of Stationary Schrödinger Equation Governing Electronic States of Quantum Dots and Rings in Magnetic Field

Marta M. Betcke[1],[*] and Heinrich Voss[2]

[1] *Department of Computer Science, University College London, Gower Street, London WC1E 6BT, UK.*
[2] *Institute of Numerical Simulation, Hamburg University of Technology, D-21071 Hamburg, Germany.*

Abstract. In this work the one-band effective Hamiltonian governing the electronic states of a quantum dot/ring in a homogenous magnetic field is used to derive a pair/quadruple of nonlinear eigenvalue problems corresponding to different spin orientations and in case of rotational symmetry additionally to quantum number $\pm\ell$. We show, that each of those pair/quadruple of nonlinear problems allows for the min-max characterization of its eigenvalues under certain conditions, which are satisfied for our examples and the common InAs/GaAs heterojunction. Exploiting the minmax property we devise efficient iterative projection methods simultaneously handling the pair/quadruple of nonlinear problems and thereby saving up to 40% of the computational time as compared to the nonlinear Arnoldi method applied to each of the problems separately.

AMS subject classifications: 65F15, 65F50

Key words: Quantum dot, quantum ring, nonlinear eigenvalue problem, minmax characterization, iterative projection method, electronic state, spin orbit interaction, magnetic field.

1 Introduction

The spectroscopic techniques involving magnetic field have for long been employed in experimental studies of bulk materials. However, only recently, methods like resonant spin-flip Raman scattering have been applied to quantum dots [30]. The analysis of Zeeman levels and the associated Landé factors allows the physicists for better understanding of spin effects on the optical response of low dimensional systems and is crucial for

---

[*]Corresponding author. *Email addresses:* `m.betcke@ucl.ac.uk` (M. M. Betcke), `voss@tu-harburg.de` (H. Voss)

interpretation of the results of spectroscopic analysis, magneto-optical experiments or magneto-transport phenomena.

In this work we consider the Zeeman splitting of energy levels of quantum dots and rings in an external homogenous magnetic field. The internal Zeeman effect i.e. the splitting of electronic levels due to the interaction of the spin magnetic moment with the magnetic field acting on the electron while it is moving around the nucleus, was considered in [5]. We discuss the general three dimensional case on an example of a pyramidal quantum dot and the rotationally symmetric case on an example of an elliptical quantum ring. We assume the one-band Hamiltonian with nonparabolic effective mass approximation and the effective Landé factor for the electronic states in the conduction band. This model yields a magnetic stationary Schrödinger equation, where the eigenvalue parameter enters nonlinearly. Considering different spin orientations we obtain a pair of nonlinear eigenvalue problems, one for each spin orientation. In case of rotational symmetry additionally each of the $\pm\ell$ quantum numbers yields a separate equation resulting in a total of four different nonlinear eigenvalue problems. We derive sufficient conditions for the physically relevant eigenvalues of the corresponding variational problems to satisfy the minmax principle [39,40]. This conditions hold for the InAs/GaAs heterojunctions in our examples. Exploiting the minmax property we develop efficient iterative projection methods which simultaneously handle the pair/quadruple of the nonlinear problems considerably reducing the overall computational time.

A standard way to tackle the rational eigenproblem (cf. [15] for a quantum dot without the magnetic field) would be to multiply it by the common denominator and to linearize the resulting polynomial of degree five. Similarly, the rational problem can be linearized directly as was proposed by Su and Bai [32]. In either case one gets a linear eigenvalue problem of dimension five times as large as the original problem. This linearized problem can then be solved with standard algorithms for which off the shelf software is available. However, this approach has some significant disadvantages. Not only the dimension of the problem is increased fivefold, but also the structure of the problem (e.g. symmetry) is destroyed and moreover the desired eigenvalues are now located in the interior of the spectrum. Computation of interior eigenvalues requires shift-invert type techniques, i.e. at least a preconditioner for the linear problem with a linearization block structure, will have to be computed. Efficient non fill-in computation of such a preconditioner is an open problem.

Our paper is organized as follows. In Section 2 we introduce the magnetic one-band effective Hamiltonian which models the electronic behavior of three dimensional quantum structures. The derivation of the corresponding pair of rational eigenvalue problems and their analysis is provided in Section 3. In Section 4 we adapt the model to a nanoring in magnetic field. Further, we derive the corresponding quadruple of nonlinear eigenvalue problems and analyze it. In Section 5 we give the minmax characterization for both problems and their discretizations obtained with Galerkin methods. The resulting rational matrix eigenvalue problems are large and sparse and therefore they can be efficiently handled by iterative projection methods like e.g. Jacobi Davidson [8] or

nonlinear Arnoldi [36], which are briefly recalled in Section 6. In Section 7 we describe modifications of the iterative projection methods tailored to simultaneously handle the pair/quadruple of nonlinear eigenvalue problems thereby considerably saving computational time. We demonstrate the efficiency of our methods on numerical examples. The conclusions together with some ideas for future research are summarized in the last section.

2   One-band effective Hamiltonian in magnetic field

We consider the magnetic one-band effective Hamiltonian for electrons in the conduction band [14, 23, 35]

$$H = (-i\hbar\nabla + eA)\frac{1}{2m(\lambda,x)}(-i\hbar\nabla + eA) + V(x) + \mu_B\frac{g(\lambda,x)}{2}\sigma B, \qquad (2.1)$$

where $\hbar$ is the reduced Planck constant, ∇ denotes the spatial gradient and $A(x)$ the vector potential such that $B = \nabla \times A(x)$ is the magnetic field intensity. Further, e and m_0 are the free electron charge and mass, $\mu_B = e\hbar/(2m_0)$ is the Bohr magneton and σ is the vector of Pauli matrices.

   We assume a constant magnetic field $B = (0,0,B)$ perpendicular to the (x,y)-plane, and we choose the symmetric gauge $A(x,y,z) = \frac{1}{2}(-By,Bx,0) \in C^\infty(\mathbb{R}^3,\mathbb{R}^3)$. We do not explicitly distinguish between the vector of the magnetic field intensity and its zth component, but the meaning will be clear from the context.

   In the effective Hamiltonian (2.1), the relations $m(\lambda,x)$ and $g(\lambda,x)$ originate from application of the $\mathbf{k}\cdot\mathbf{p}$ theory (see [3,9,16] for general introduction). In $\mathbf{k}\cdot\mathbf{p}$ framework, each eigenfunction of one electron Schrödinger equation in a periodic crystal potential is represented using Bloch's theorem as a product of a periodic envelope function and a plane wave $\exp(i\mathbf{k}\cdot\mathbf{r})$. This representation is then used to reduce the one electron Schrödinger equation to a Hamiltonian acting on the envelope functions. In this process the eponymous nondiagonal term, $\mathbf{k}\cdot\mathbf{p}$, is introduced, which however for small $\mathbf{k}$ can be treated as a perturbation of the diagonal of the Hamiltonian. Using second order perturbation theory, the linear term can be absorbed into the effective coefficients. The linearity in $\mathbf{k}$ of the $\mathbf{k}\cdot\mathbf{p}$ term contravenes the parabolic dispersion relation of the free electron $\hbar^2 k^2/(2m_0)$, which is rectified using effective coefficients.

   In presence of a homogenous magnetic field, the momentum $\mathbf{p}$ is the kinetic momentum $(-i\hbar\nabla + eA)$. Moreover, the Hamiltonian contains an additional term, $\frac{1}{2}g_0\mu_B\sigma B$, describing the interaction of the spin angular momentum with the magnetic field, where $g_0 \approx 2$ is the g-Landé factor of the free electron. Applying the $\mathbf{k}\cdot\mathbf{p}$ theory to the kinetic momentum, the 0th order in A terms result in the effective mass as given in (2.2), while the terms linear in A yield the effective g-factor (2.3), [23].

   The electron effective mass $m(\lambda,x)$ [3, 9] is constant on the dot $\Omega_q \subset \mathbb{R}^3$ and on the

surrounding matrix $\Omega_m \subset \mathbb{R}^3$ for every fixed energy level λ

$$\frac{1}{m_j(\lambda)} := \frac{1}{m(\lambda,x)}\bigg|_{x\in\Omega_j} = \frac{P_j^2}{\hbar^2}\left(\frac{2}{\lambda+E_{g,j}-V_j} + \frac{1}{\lambda+E_{g,j}-V_j+\Delta_j}\right), \quad j\in\{q,m\}. \qquad (2.2)$$

Here the confinement potential $V_j := V|_{\Omega_j}$ is piecewise constant, and P_j, $E_{g,j}$ and Δ_j are the momentum matrix element, the band gap, and the spinorbit splitting in the valence band for the quantum dot material ($j=q$) and the matrix ($j=m$), respectively. The values of the semiconductor parameters are summarized in Table 1. It is known that pyramid shape dots are under significant degree of strain, which in turn affects their electronic levels. Therefore for simulations with pyramidal shapes we adopted a strain model based on "model-solid approach" of Van der Walle and Martin [7,33] resulting in strained values of the band gap E_p and the confinement potential V.

Table 1: Semiconductor parameters, values without and with strain.

	P	Δ	E_g	V	strained E_g	strained V
InAs	0.7509	0.48	0.42	0	0.943	0
GaAs	0.7848	0.34	1.52	0.77	1.52	0.395

The effective Landé factor $g(\lambda,x)$ [14,23,35] in (2.1) is given by the following equation

$$g_j(\lambda) := g(\lambda,x)|_{x\in\Omega_j} = 2\left\{1 - \frac{m_0}{m_j(\lambda)}\frac{\Delta_j}{3(\lambda+E_{g,j}-V_j)+2\Delta_j}\right\}, \quad j\in\{q,m\}. \qquad (2.3)$$

Analogously to the effective mass, for a fixed energy level λ, $g(\lambda,x)$ is a piecewise constant function.

Under these assumptions the energy states and the corresponding wave functions for electrons are obtained from the Schrödinger equation

$$\frac{1}{2m_j(\lambda)}(-i\hbar\nabla+eA(x))^2\Phi+V_j\Phi+\mu_B\frac{g_j(\lambda)}{2}\sigma B\Phi=\lambda\Phi, \quad j\in\{q,m\}. \qquad (2.4)$$

For physical applications the interesting eigenvalues are those in the interval (V_q,V_m). These are also called confined states, since the corresponding wave functions Φ live mainly on the quantum structure and decay rapidly outside of the structure. For this reason it is appropriate to consider the eigenvalue problem on a bounded matrix domain Ω_m with homogenous Dirichlet conditions on the outer boundary of the matrix. On the interface between the dot and the matrix the electron wave functions are continuous and since $A(x)\in C^\infty(\mathbb{R}^3,\mathbb{R}^3)$ the Ben Daniel-Duke condition is appropriate [3,35]

$$\frac{1}{m_q(\lambda)}\frac{\partial\Phi(x)}{\partial\bar{n}_q} = \frac{1}{m_m(\lambda)}\frac{\partial\Phi(x)}{\partial\bar{n}_m}, \quad x\in\partial\Omega_{int},$$

where $\partial\Omega_{int} = \partial\Omega_q \cap \partial\Omega_m$ and $\bar{n}_q$ and $\bar{n}_m$ denotes the outward normal vector of the dot and the matrix, respectively.

In this work we focus on two models: a fully three dimensional quantum dot model and an axially symmetric quantum ring model. The fully three dimensional case is considered in Section 3. The second model allows for the separation of the angular direction hence resulting in equation with a different structure which is handled separately in Section 4. We would like to point out that the ideas presented in this work can also be applied to more general structures in particular to quantum dots on wetting layers and to arrays of quantum dots with or without the axial symmetry.

3 Quantum dot in magnetic field

First, we consider a quantum dot $\Omega_q \subset \mathbb{R}^3$ embedded into a cuboid matrix $\Omega_m \subset \mathbb{R}^3$, which is exposed to a homogenous magnetic field (cf. Fig. 1).
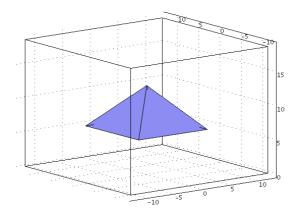

Figure 1: Pyramidal quantum dot embedded in a cuboid matrix.

We recall that the eigenvalues of physical relevance are those below the confinement potential. Therefore, for the sake of simplicity we gauge the potential $V_q = 0$, so that the relevant eigenvalues are in the interval $J := (0, V_m)$. In this section we derive the characterization of these eigenvalues as the minmax values of a Rayleigh functional.

Let $\Omega := \overline{\Omega}_q \cup \Omega_m$. An appropriate space for the magnetic Schrödinger equation with the vector potential A and Dirichlet boundary conditions on $\partial\Omega$ is (cf. [10, 22])

$$\mathcal{H} := \left\{ \phi : \Omega \to \mathbb{C} : \phi \in L^2(\Omega), \, (\nabla + i\tilde{A})\phi \in L^2(\Omega), \, \phi = 0 \text{ on } \partial\Omega \right\}$$

with $\tilde{A} := \frac{e}{\hbar} A$ and the associated inner product

$$\langle \phi, \psi \rangle := \int_\Omega (\nabla + i\tilde{A})\phi \cdot \overline{(\nabla + i\tilde{A})\psi} dx. \tag{3.1}$$

By virtue of the diamagnetic inequality [22]

$$|\nabla|\phi|(x)| \leq |(\nabla+i\tilde{A})\phi(x)| \quad \text{for all } \phi \in \mathcal{H} \text{ and a.e. } x \in \Omega$$

and Friedrich's inequality for $|\phi|$, the induced norm $\|\phi\|$ is equivalent to the Sobolev norm in $H_0^1(\Omega)$. Therewith $\mathcal{H}$ is compactly embedded in $L^2(\Omega)$ along with $H^1(\Omega)$. The details of the argument are given in [1,4].

Now, we are in the position to set up the variational form of the Schrödinger equation. Multiplying (2.4) with $\bar{\psi}$ and integrating over Ω we arrive at

$$a_{\pm}(\phi,\psi;\lambda) := \frac{\hbar^2}{2m_q(\lambda)} \int_{\Omega_q} (\nabla+i\tilde{A})\phi \cdot \overline{(\nabla+i\tilde{A})\psi} dx + \frac{\hbar^2}{2m_m(\lambda)} \int_{\Omega_m} (\nabla+i\tilde{A})\phi \cdot \overline{(\nabla+i\tilde{A})\psi} dx$$

$$+ V_m \int_{\Omega_m} \phi\bar{\psi} dx \pm \left(\gamma_q^B(\lambda) \int_{\Omega_q} \phi\bar{\psi} dx + \gamma_m^B(\lambda) \int_{\Omega_m} \phi\bar{\psi} dx \right)$$

$$= \lambda \int_{\Omega} \phi\bar{\psi} dx =: \lambda b(\phi,\psi) \quad \forall \psi \in \mathcal{H}, \tag{3.2}$$

where $\gamma_j^B(\lambda) = \frac{1}{2}\mu_B B g_j(\lambda)$, and its sign accounts for different spin orientations in the magnetic field along the z axis.

The quadratic form $b(\cdot,\cdot)$ obviously is sesquilinear, positive, and bounded on $L^2(\Omega)$. Under the assumption $E_{g,j} - V_j > 0$ the functions $\lambda \mapsto 1/m_j(\lambda)$ are defined for $\lambda \geq 0$, and are positive and monotonically decreasing. Moreover, $g_j(\lambda)$ and therewith $\gamma_j^B(\lambda)$ are monotonically increasing for $B > 0$ and bounded on J. Hence $a_{\pm}(\cdot,\cdot;\lambda)$ is a sesquilinear and bounded form.

If $B = 0$, i.e. in the absence of the magnetic field, $\gamma_j^B(\lambda) = 0$ for $j = \{q,m\}$ and there is no level splitting. Problems of this type were investigated in [4,7,24,38] and the minmax characterization is given therein.

For $B \neq 0$ the ellipticity can not be argued unconditionally as in the case $B = 0$. The following lemma contains a sufficient condition for $a_{\pm}(\cdot,\cdot;\lambda)$ to be $\mathcal{H}$-elliptic for all $\lambda \in J$ such that each of the linear eigenvalue problems

$$\text{Find } \mu^{\pm} \text{ and } \phi \in \mathcal{H}, \ \phi \neq 0 \text{ with } a_{\pm}(\phi,\psi;\lambda) = \mu^{\pm} b(\phi,\psi) \quad \forall \psi \in \mathcal{H} \tag{3.3}$$

has a countable set of eigenvalues $0 < \mu_1^{\pm}(\lambda) \leq \mu_2^{\pm}(\lambda) \leq \cdots$ which can be characterized by the minmax principle of Poincaré

$$\mu_j^{\pm}(\lambda) = \min_{\dim V = j, V \subset \mathcal{H}} \max_{\phi \in V, \phi \neq 0} \frac{a_{\pm}(\phi,\phi;\lambda)}{b(\phi,\phi)}.$$

Lemma 3.1. *Let $\kappa_{\min}$ be the smallest eigenvalue of the following linear eigenvalue problem*

$$c(\phi,\psi):=\int_{\Omega}(\nabla+i\tilde{A})\phi\cdot\overline{(\nabla+i\tilde{A})\psi}\,dx=\kappa\int_{\Omega}\phi\bar{\psi}\,dx \quad \forall\psi\in\mathcal{H}. \tag{3.4}$$

If the following condition is satisfied,

$$\min\left\{\frac{\hbar^2}{2m_q(\lambda)},\frac{\hbar^2}{2m_m(\lambda)}\right\} > \frac{\max\{|\gamma_q^B(\lambda)|,|\gamma_m^B(\lambda)|-V_m\}}{\kappa_{min}} \quad \forall\lambda\in J, \tag{3.5}$$

then $a_{\pm}(\cdot,\cdot;\lambda)$ is $\mathcal{H}$-elliptic for every fixed $\lambda\in J$.

Proof. For $\phi\in\mathcal{H}$ it holds that

$$
\begin{aligned}
a_{\pm}(\phi,\phi;\lambda) &\geq \min\left\{\frac{\hbar^2}{2m_q(\lambda)},\frac{\hbar^2}{2m_m(\lambda)}\right\}c(\phi,\phi)-\max\{|\gamma_q^B(\lambda)|,|\gamma_m^B(\lambda)|-V_m\}\int_{\Omega}|\phi|^2dx\\
&\geq \left(\min\left\{\frac{\hbar^2}{2m_q(\lambda)},\frac{\hbar^2}{2m_m(\lambda)}\right\}-\frac{\max\{|\gamma_q^B(\lambda)|,|\gamma_m^B(\lambda)|-V_m\}}{\kappa_{min}}\right)c(\phi,\phi)\\
&= \left(\min\left\{\frac{\hbar^2}{2m_q(\lambda)},\frac{\hbar^2}{2m_m(\lambda)}\right\}-\frac{\max\{|\gamma_q^B(\lambda)|,|\gamma_m^B(\lambda)|-V_m\}}{\kappa_{min}}\right)\|\phi\|^2.
\end{aligned}
$$

This completes the proof of the lemma. □

We remark that for $B=0$ the right hand side of (3.5) becomes 0 and since $\frac{\hbar^2}{2m_j(\lambda)}>0$, $j\in\{q,m\}$ the condition is trivially satisfied, which is consistent with the earlier results in [4,7,24,38].

Variational characterizations for the linear eigenproblem $a(\phi,\psi)=\lambda b(\phi,\psi)$ employ the Rayleigh quotient $R(\phi):=a(\phi,\phi)/b(\phi,\phi)$ which is the unique solution of the real equation $f(\lambda;\phi)=\lambda b(\phi,\phi)-a(\phi,\phi)$. More generally, a variational characterization of real eigenvalues of a nonlinear eigenvalue problem like (3.2) requires a Rayleigh functional, which is defined as a solution of the corresponding equation

$$f_{\pm}(\lambda;\phi):=\lambda b(\phi,\phi)-a_{\pm}(\phi,\phi;\lambda)=0. \tag{3.6}$$

The following lemma contains a sufficient condition for the existence of such a Rayleigh functional.

Lemma 3.2. *Assume that the conditions of* Lemma 3.1 *hold, and*

$$-\frac{\hbar^2}{2}\max\left\{\left(\frac{1}{m_q(\lambda)}\right)',\left(\frac{1}{m_m(\lambda)}\right)'\right\} > \frac{\max\{|\gamma_q'^B(\lambda)|,|\gamma_m'^B(\lambda)|\}-1}{\kappa_{\min}}, \tag{3.7}$$

for every $\lambda \in J$, where $\kappa_{\min}$ denotes the smallest eigenvalue of the eigenvalue problem (3.4). Then for every $\phi \in \mathcal{H}$, $\phi \neq 0$ each of the real functions $f_\pm$ satisfies

$$f_\pm(0;\phi) < 0 \quad and \quad \frac{\partial}{\partial\lambda} f_\pm(\lambda;\phi) > 0 \quad \forall \lambda \in J.$$

Hence, Eq. (3.6) implicitly defines a Rayleigh functional $p_\pm : \mathcal{H} \supset D_\pm \to J$ for each of the eigenproblems (3.2) where $D_\pm := \{\phi \in \mathcal{H} : f_\pm(\lambda;\phi) = 0 \text{ solvable in } J\}$.

Proof. $f_\pm(0;\phi) = -a_\pm(\phi,\phi;0) < 0$ follows immediately from the ellipticity of $a_\pm(\cdot,\cdot;0)$. For every $\phi \in \mathcal{H}$, $\phi \neq 0$ and every $\lambda \in J$ it holds that

$$\frac{\partial}{\partial\lambda} f_\pm(\lambda;\phi) = -\left(\frac{\hbar^2}{2m_q(\lambda)}\right)' \int_{\Omega_q} |(\nabla + i\tilde{A})\phi|^2 dx - \left(\frac{\hbar^2}{2m_q(\lambda)}\right)' \int_{\Omega_m} |(\nabla + i\tilde{A})\phi|^2 dx$$

$$\mp \left(\gamma_q'^B(\lambda) \int_{\Omega_q} |\phi|^2 dx + \gamma_m'^B(\lambda) \int_{\Omega_m} |\phi|^2 dx\right) + \int_{\Omega} |\phi|^2 dx$$

$$\geq -\max\left\{\left(\frac{\hbar^2}{2m_q(\lambda)}\right)', \left(\frac{\hbar^2}{2m_m(\lambda)}\right)'\right\} c(\phi,\phi) - \left(\max\{|\gamma_q'^B(\lambda)|, |\gamma_m'^B(\lambda)|\} - 1\right) \int_{\Omega} |\phi|^2 dx. \quad (3.8)$$

Here we need to consider two cases:

$$\max\{|\gamma_q'^B(\lambda)|, |\gamma_m'^B(\lambda)|\} \leq 1 \quad and \quad \max\{|\gamma_q'^B(\lambda)|, |\gamma_m'^B(\lambda)|\} > 1.$$

In the first case the second term becomes nonpositive, which immediately implies that the entire expression is positive completing the argument. Moreover, case 1 also implies the condition (3.7), as the left hand side of (3.7) is always positive on J due to the functions $1/m_j(\lambda)$ for $j \in \{q,m\}$ being monotonically falling.

In the second case we complete the above argument bounding (3.8) from below by

$$\left(-\max\left\{\left(\frac{\hbar^2}{2m_q(\lambda)}\right)', \left(\frac{\hbar^2}{2m_m(\lambda)}\right)'\right\} - \frac{\max\{|\gamma_q'^B(\lambda)|, |\gamma_m'^B(\lambda)|\} - 1}{\kappa_{min}}\right) c(\phi,\phi) > 0,$$

where (3.7) has been used. $\square$

We remark that for $B = 0$,

$$\max\{|\gamma_q'^B(\lambda)|, |\gamma_m'^B(\lambda)|\} = 0 < 1,$$

implying the existence of the Rayleigh functional. Therefore also this condition is consistent with the previous results.

It follows from [39, 40] that the eigenvalues of (3.2) in $J = (0, V_m)$ allow a minmax characterization. In general, the eigenvalues of a nonlinear eigenvalue problem have to be specially enumerated for the minmax characterization to hold. However, this ordering coincides with the natural ascending ordering, if the infimum of the Rayleigh functional is contained in J.

Lemma 3.3. *Assume that the conditions of* Lemma 3.2 *are satisfied. Then it holds that*

$$\inf_{\phi \in D_\pm} p_\pm(\phi) > 0. \tag{3.9}$$

Proof. Let $\mu_1^\pm(\lambda)$ be the smallest eigenvalue of (3.3). Then $\mu_1^\pm(0) > 0$, and by the continuous dependence of $\mu_1^\pm(\lambda)$ on λ there exists $\varepsilon > 0$ such that

$$\frac{a_\pm(\phi,\phi;\varepsilon)}{b(\phi,\phi)} \geq \mu_1^\pm(\varepsilon) > \frac{1}{2}\mu_1^\pm(0) > 0 \quad \text{for every } \phi \in \mathcal{H}, \phi \neq 0.$$

Let $\mu_0^\pm := \min(\varepsilon, 0.5\mu_1^\pm(0))$. Then it follows from the monotonicity of $a_\pm(\phi,\phi;\lambda)$ that

$$f(\mu_0^\pm;\phi) = \mu_0^\pm b(\phi,\phi) - a(\phi,\phi;\mu_0^\pm) < 0 \quad \text{for every } \phi \in \mathcal{H}, \phi \neq 0,$$

which in turn implies $p_\pm(\phi) > \mu_0^\pm > 0$ for every $\phi \in D_\pm$. Hence (3.9) holds and therewith $\inf_{\phi \in D_\pm} p_\pm(\phi) \in J$. □

In the next section we proceed to give an equivalent analysis for the rotationally symmetric problem before finally stating the minmax principle for both problems in Section 5.

4　Axially symmetric Hamiltonian

In this section we derive the stationary Schrödinger equation governing electronic levels of axially symmetric quantum structures. Due to the symmetry we can separate off the angular direction and consider a sequence of two dimensional problems in the (r,z) plane instead. For the plane problem let $\Omega, \Omega_q, \Omega_m$ and the boundaries $\partial\Omega, \partial\Omega_q, \partial\Omega_m$ denote their restrictions to the (r,z) plane. We consider an elliptical quantum ring, Ω_q, obtained by a revolution around the z-axis of an ellipse centered at (r_0, z_0) with principal axes a (along the r-axis) and b (along z-axis), centrally embedded in a cylindrical matrix, Ω_m, of radius R_m and height Z_m. The quantum ring and the matrix are displayed in Fig. 2.

To separate the angular direction we rewrite the stationary Schrödinger equation (2.4) in cylindrical coordinates choosing the gauge $A = \frac{1}{2}(B \times \mathbf{r})$, where $\mathbf{r}$ denotes the point vector (θ, r, z)

$$-\frac{\hbar^2}{2m_j(\lambda)}\left[\frac{1}{r}\frac{\partial}{\partial r}\left(r\frac{\partial\Phi}{\partial r}\right) + \frac{1}{r^2}\frac{\partial^2\Phi}{\partial\theta^2} + \frac{\partial^2\Phi}{\partial z^2}\right] + \frac{e^2}{8m_j(\lambda)}(B \times \mathbf{r})^2$$

$$-\frac{i\hbar e}{2m_j(\lambda)}(B \times \mathbf{r})\cdot\nabla\Phi + \sigma_z\frac{\mu_B}{2}Bg_j(\lambda)\Phi + V_j\Phi = \lambda\Phi, \quad j \in \{q,m\}. \tag{4.1}$$

Due to the radial symmetry of the problem we expect a solution of the following type

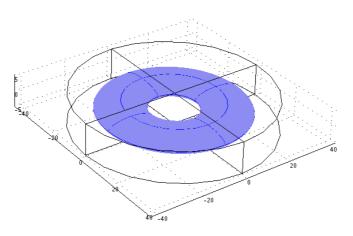$$\Phi(\theta,r,z) = \phi(r,z)\psi(\theta). \tag{4.2}$$

Figure 2: Elliptical quantum ring embedded in a cylindrical matrix.

Substituting (4.2) in (4.1) and separating the variables we obtain two independent equations [35]

$$\frac{\hbar^2}{2m_j(\lambda)}\left[\frac{\partial}{\partial r}\left(-r\frac{\partial\phi(r,z)}{\partial r}\right)-r\frac{\partial^2\phi(r,z)}{\partial z^2}+\frac{\ell^2}{r}\phi(r,z)\right]+\frac{e^2B^2}{8m_j(\lambda)}r^3\phi(r,z)$$

$$+\ell B\frac{\hbar e}{2m_j(\lambda)}r\phi(r,z)+\sigma_z\frac{\mu_B}{2}Bg_j(\lambda)r\phi(r,z)+(V_j-\lambda)r\phi(r,z)=0, \qquad (4.3)$$

$$\frac{\partial^2\psi(\theta)}{\partial\theta^2}+\ell^2\psi(\theta)=0. \qquad (4.4)$$

Here we made use of the definition of the angular momentum

$$L=\mathbf{r}\times(-i\hbar\nabla)$$

along with the fact that its projection on the z-axis is quantized by the angular quantum number ℓ, i.e. $L\cdot B=\ell\hbar B$.

The solution of the second equation (4.4) is well known to be a plane wave

$$\psi_\ell(\theta)=\exp(i\ell\theta), \quad \ell=0,\pm1,\pm2,\cdots,$$

while the first equation (4.3) is a nonlinear eigenvalue problem in the plane defined by r and z.

On the outer boundary of the matrix, $\partial\Omega$, the homogeneous Dirichlet conditions, and on the dot matrix interface, Ω_{int}, the BenDaniel-Duke conditions are inherited from the three dimensional problem. On the rotational axis, $\partial\Omega_{rot}$, for continuity reasons we assume homogeneous Neumann conditions $\partial\phi/\partial r=0$ for $\ell=0$ and homogeneous Dirichlet conditions $\phi=0$ for $\ell\neq0$.

The eigenvalues of each of the three dimensional problems (4.1) with $\sigma_z=\pm1$, respectively, are ordered eigenvalues of the sequence of two dimensional problems (4.3)

corresponding to the quantum numbers $\ell=0,\pm1,\pm2,\cdots$. The eigenfunctions of (4.1) have the following form

$$\Phi(\theta,r,z) = \phi_{\ell,\sigma_z}(r,z)\exp(i\ell\theta),$$

where $\phi_{\ell,\sigma_z}(r,z)$ is an eigenfunction of the corresponding plane problem. Henceforth for simplicity of notation we omit the index indicating the dependence of the eigenfunction on ℓ and σ_z.

In the presence of magnetic field the electronic levels split, which leads to a pair for $\ell=0$ and a quadruple for $\ell\neq0$ of plane problems to be solved which differ by the sign of the third and fourth terms in (4.3). Problems of this type were also numerically investigated by other authors by means of Full Approximation Methods (FAM) [12, 19–21, 34], which are substantially less efficient than the iterative projection methods presented here. For comparison of FAM type methods with iterative projection methods see Section 4.3 in [4]. In contrast without the magnetic field, $B=0$, there is only one problem to solve for each $|\ell|$. The iterative projection methods for rotationally symmetric quantum dots in the absence of magnetic field are discussed in Chapter 4 of [4].

We now proceed to give an analysis for the axially symmetric problem analogous to that of the general three dimensional case in Section 3.

Let $\Omega:=(0,R_m)\times(-Z_m/2,Z_m/2)$, $\Omega_q:=\{(r,z):(r-r_0)^2/a^2+(z-z_0)^2/b^2<1\}$, and $\Omega_m:=\Omega\setminus\bar{\Omega}_q$. Due to the term ℓ^2/r it is necessary to distinguish two cases $\ell=0$ and $\ell\neq0$, since the trial function spaces in the variational formulation are different.

For $\ell=0$, since the splitting of the energy levels is only due to the Zeeman term, it is appropriate to describe the problem in the weighted Sobolev space

$$\mathcal{H}_0 := \left\{ \phi \in L^2(\Omega) : r|\nabla\phi|^2 \in L^1(\Omega), \quad \begin{array}{ll} \phi(r,\pm Z_m/2)=0, & 0\leq r \leq R_m, \\ \phi(R_m,z)=0, & -Z_m/2\leq z \leq Z_m/2 \end{array} \right\}$$

with the scalar product

$$\langle\phi,\psi\rangle_{\mathcal{H}_0} := \int_\Omega r\nabla\phi\cdot\nabla\psi d(r,z),$$

and the weighted Lebesgue space

$$\mathcal{W} := \{\phi : r|\phi|^2 \in L^1(\Omega)\} \quad \text{with} \quad \langle\phi,\psi\rangle_{\mathcal{W}} := \int_\Omega r\phi\psi d(r,z).$$

Then $\mathcal{H}_0$ is compactly embedded in $\mathcal{W}$ (cf. [29], Theorem. 7.13(ii), Remark 7.14(i)).

For $\ell\neq0$ the following environment is appropriate. Let $\mathcal{H}_\ell$ be the weighted Sobolev space

$$\mathcal{H}_\ell = H_0^1(\Omega;r^{-1},r) := \left\{ \phi : \frac{1}{r}|\phi|^2 \in L^1(\Omega), r|\nabla\phi|^2 \in L^1(\Omega), \quad \phi=0 \text{ on } \partial\Omega \right\}$$

with the standard inner product

$$\langle\phi,\psi\rangle_{\mathcal{H}_\ell} := \int_\Omega r\nabla\phi\cdot\nabla\psi + \frac{1}{r}\phi\psi d(r,z)$$

and we define $\mathcal{W}$ as in case $\ell=0$. Then by [29], Theorem. 18.12 and Example. 18.15, $\mathcal{H}_\ell$ is compactly embedded in $\mathcal{W}$. For the details of both embedding arguments see Section 4.2 of [4].

For the simplicity of the notation, from now on we refer to the appropriate trial function space using the conditional space definition

$$\mathcal{H} := \left\{ \begin{array}{ll} \mathcal{H}_0, & \ell=0, \\ \mathcal{H}_\ell, & \ell\neq 0. \end{array} \right.$$

Multiplying equation (4.3) by $\psi\in\mathcal{H}$ and integrating by parts, we obtain the variational form of the Schrödinger equation (4.3)

Find $\lambda\in J$ and $\phi\in\mathcal{H}$, $\phi\neq 0$ such that

$$a_\pm^\ell(\phi,\psi;\lambda) := \frac{\hbar^2}{2m_q(\lambda)} \int_{\Omega_q} \left(r\nabla\phi\cdot\nabla\psi + \frac{\ell^2}{r}\phi\psi + \frac{\mathcal{B}^2}{4}r^3\phi\psi \right) d(r,z)$$

$$+ \frac{\hbar^2}{2m_m(\lambda)} \int_{\Omega_m} \left(r\nabla\phi\cdot\nabla\psi + \frac{\ell^2}{r}\phi\psi + \frac{\mathcal{B}^2}{4}r^3\phi\psi \right) d(r,z)$$

$$\pm \left(\gamma_q^B(\lambda) \int_{\Omega_q} r\phi\psi d(r,z) + \gamma_m^B(\lambda) \int_{\Omega_m} r\phi\psi d(r,z) \right)$$

$$\pm |\ell\mathcal{B}| \left(\frac{\hbar^2}{2m_q(\lambda)} \int_{\Omega_q} r\phi\psi d(r,z) + \frac{\hbar^2}{2m_m(\lambda)} \int_{\Omega_m} r\phi\psi d(r,z) \right) + V_m \int_{\Omega_m} r\phi\psi d(r,z)$$

$$= \lambda \int_\Omega r\phi\psi d(r,z) =: \lambda b(\phi,\psi) \quad \forall\psi\in\mathcal{H}, \tag{4.5}$$

where $\mathcal{B}=eB/\hbar$ and $\gamma_j^B(\lambda)$ were defined in Section 3.

The bilinear form $b(\cdot,\cdot)$ is obviously positive and bounded on $\mathcal{W}$. The bilinear form $a_\pm^\ell(\cdot,\cdot;\lambda)$ is symmetric and the boundedness immediately follows from the compact embedding of $\mathcal{H}$ into $\mathcal{W}$ and the boundedness of $\lambda\mapsto\frac{1}{m_j(\lambda)}$ and $\gamma_j^B(\lambda)$ on J.

Lemma 4.1 gives a sufficient condition for $a_\pm^\ell(\cdot,\cdot;\lambda)$, to be $\mathcal{H}$-elliptic, thus for a fixed $\lambda\in J$ the linear eigenvalue problem

Find μ^ℓ and $\phi\in\mathcal{H}$, $\phi\neq 0$ with $a_\pm^\ell(\phi,\psi;\lambda)=\mu^\ell b(\phi,\psi)$ for every $\psi\in\mathcal{H}$

has a countable set of eigenvalues $0<\mu_1^{\ell\pm}\leq\mu_2^{\ell\pm}\leq\cdots$ which can be characterized as min-max values of the Rayleigh quotient (cf. (3.3)).

The proofs of Lemmata 4.1 and 4.2 follow the same lines as Lemmata 3.1 and 3.2 and are therefore omitted, for details we refer to [6].

Lemma 4.1. *Let $\kappa_{\min}$ be the smallest eigenvalue of the following eigenvalue problem*

$$c^\ell(\phi,\psi):=\int_\Omega \left(r\nabla\phi\cdot\nabla\psi+\frac{\ell^2}{r}\phi\psi+\frac{\mathcal{B}^2}{4}r^3\phi\psi \right)d(r,z)=\kappa\int_\Omega r\phi\psi d(r,z) \qquad (4.6)$$

for every $\psi\in\mathcal{H}$. If

$$\min\left\{ \frac{\hbar^2}{2m_q(\lambda)},\frac{\hbar^2}{2m_m(\lambda)} \right\} > \frac{\max\{\omega_q^B(\lambda),\omega_m^B(\lambda)\}}{\kappa_{min}} \quad \forall\lambda\in J, \qquad (4.7)$$

where

$$\omega_j^B(\lambda)=|\gamma_j^B(\lambda)|-V_j+|\ell\mathcal{B}|\frac{\hbar^2}{2m_j(\lambda)},$$

then $a_\pm^\ell(\cdot,\cdot;\lambda)$ is $\mathcal{H}$-elliptic for every fixed $\lambda\in J$.

As in Section 3 we require the existence of a Rayleigh functional $p_\pm^\ell$, which is a solution of the corresponding equation

$$f_\pm^\ell(\lambda;\phi):=\lambda b(\phi,\phi)-a_\pm^\ell(\phi,\phi;\lambda)=0.$$

The sufficient condition for its existence is given by the following lemma.

Lemma 4.2. *Assume that the conditions of* Lemma 4.1 *hold, and*

$$-\frac{\hbar^2}{2}\max\left\{ \left(\frac{1}{m_q(\lambda)}\right)',\left(\frac{1}{m_m(\lambda)}\right)' \right\} > \frac{\max\{\eta_q^B(\lambda),\eta_m^B(\lambda)\}-1}{\kappa_{\min}} \quad \forall\lambda\in J, \qquad (4.8)$$

where

$$\eta_j^B(\lambda)=|\gamma_j'^B(\lambda)|-|\ell\mathcal{B}|\left(\frac{\hbar^2}{2m_j(\lambda)}\right)'$$

and $\kappa_{\min}$ denotes the smallest eigenvalue of the eigenvalue problem (4.6). *Then for every $\phi\in\mathcal{H}$, $\phi\neq0$ each of the real equations*

$$f_\pm^\ell(\lambda;\phi):=\lambda b(\phi,\phi)-a_\pm^\ell(\phi,\phi;\lambda)=0$$

has at most one solution $p_\pm^\ell(\phi)\in J$ and $\inf_{\phi\in D_\pm^\ell}p_\pm^\ell(\phi)\in J$ for the domain of definition $D_\pm^\ell\subset \mathcal{H}\setminus\{0\}$ of $p_\pm^\ell$.

5 Minmax principle

Finally, we are in the position to formulate the minmax principle for both nonlinear eigenvalue problems (3.2) and (4.5). For the compactness of notation we henceforth drop the superscript ℓ for the plane problem.

Under the conditions of Lemma 3.2 or Lemma 4.2 for each of the eigenvalue problems in (3.2) and (4.5), the Rayleigh functional

$$p_\pm : \mathcal{H} \supset D_\pm \to J$$

is defined. The general conditions of the minmax theory for nonlinear eigenvalue problems in [40] are satisfied, and Theorems 2.1 and 2.9 of [40] imply the following characterization of the eigenvalues of (3.2) and (4.5) in the interval J.

Theorem 5.1. *Assume that the conditions of* Lemma 3.2 *or* Lemma 4.2, *respectively, are satisfied. Then each of the Schrödinger equations in* (3.2) *and* (4.5), *has a finite number of eigenvalues in J, and it holds that*

(i) The kth smallest eigenvalue can be characterized by

$$\lambda_k^\pm = \min_{\dim V = k,\ V \cap D_\pm \neq \varnothing} \max_{\phi \in V \cap D_\pm} p_\pm(\phi). \tag{5.1}$$

(ii) The minimum in (5.1) *is attained for the subspace which is spanned by eigenfunctions corresponding to the k smallest eigenvalues of the linear eigenproblem*

$$a_\pm(\phi,\psi;\lambda_k^\pm) = \mu b(\phi,\psi), \quad \forall \psi \in \mathcal{H}. \tag{5.2}$$

Remark 5.1. Notice, that the kth largest eigenvalue of the linear problem,

$$\lambda b(\phi,\psi) - a_\pm(\phi,\psi,\lambda) = \nu b(\phi,\psi), \quad \forall \psi \in \mathcal{H},$$

obtained from the nonlinear problem through fixing the parameter λ, corresponds to the kth smallest eigenvalue of the linear problem in its common form (5.2).

Equipped with this result we can devise efficient iterative projection methods which compute approximations to the eigenvalues of the nonlinear problem safely one after another and without repeated convergence to already computed eigenpairs, as it can be achieved in the linear case. To apply numerical methods we discretize the Schrödinger equations by a Rayleigh-Ritz method (e.g. finite elements). For the three dimensional problem we obtain a rational matrix eigenvalue problem of the following type

$$
\begin{aligned}
S_\pm(\lambda)x := \lambda M x &- \frac{\hbar^2}{2m_q(\lambda)} K_q x - \frac{\hbar^2}{2m_m(\lambda)} K_m x - V_m M_m x \\
&\pm (\gamma_q^B(\lambda) M_q + \gamma_m^B(\lambda) M_m) x = 0,
\end{aligned}
\tag{5.3}
$$

and the involved matrices are given by the integrals of the products of the shape functions ϕ_k, $k \in 1, \cdots, n$ and their derivates

$$K_j^{(k,l)} = \int\limits_{\Omega_j} (\nabla + i\tilde{A})\phi_k \overline{(\nabla + i\tilde{A})\phi_l}\, dx, \quad j \in \{q,m\},$$

$$M^{(k,l)} = \int\limits_{\Omega} \phi_k \bar{\phi}_l\, dx \quad \text{and} \quad M_j^{(k,l)} = \int\limits_{\Omega_j} \phi_k \bar{\phi}_l\, dx.$$

In the axially symmetric case we arrive at the following rational matrix eigenvalue problem

$$S_\pm^\ell(\lambda)x := \lambda Mx - \frac{\hbar^2}{2m_q(\lambda)}K_q x - \frac{\hbar^2}{2m_m(\lambda)}K_m x - V_m M_m x$$

$$\pm(\gamma_q^B(\lambda)M_q + \gamma_m^B(\lambda)M_m)x \pm |\ell\mathcal{B}|\left(\frac{\hbar^2}{2m_q(\lambda)}M_q + \frac{\hbar^2}{2m_m(\lambda)}M_m\right)x = 0, \quad (5.4)$$

where

$$K_j^{(k,l)} = \int\limits_{\Omega_j}\left(r\nabla\phi_k\nabla\phi_l + \frac{\ell^2}{r}\phi_k\phi_l + \frac{\mathcal{B}^2}{4}r^3\phi_k\phi_l\right)d(r,z), \quad j \in \{q,m\},$$

$$M^{(k,l)} = \int\limits_{\Omega}r\phi_k\phi_l d(r,z) \quad \text{and} \quad M_j^{(k,l)} = \int\limits_{\Omega_j}r\phi_k\phi_l d(r,z).$$

The following corollary is an obvious consequence of the Theorem 5.1, where we again skipped the superscript ℓ for the compactness of notation.

Corollary 5.1. *For each of the discretized problems in (5.3) and (5.4) the discrete versions of the conditions of Lemmas 3.2 and 4.2, respectively, are sufficient for the existence of Rayleigh functionals $q_\pm$ corresponding to $S_\pm$ on the interval J, and the eigenvalues of $S_\pm$ in J are minmax values of $q_\pm$. Moreover, it follows from the minmax characterization that the kth smallest eigenvalue of $S_\pm$ is an upper bound for the corresponding eigenvalue of the original continuous problem in (3.2) and (4.5), respectively.*

6 Solving the nonlinear eigenvalue problem

In this section we consider the problem to compute a few eigenvalues and the corresponding eigenvectors at the lower end of the spectrum of the discretization (5.3) or (5.4) of the Schrödinger equation. Since the described numerical methods apply to all of the discrete problems $S_\pm, S_\pm^\ell$ in the remainder of this section we omit any sub- and superscripts and refer to the discretized eigenvalue problem to be solved by $S(\lambda)x = 0$.

An established tool for solution of large scale linear sparse eigenproblems are iterative projection methods like for instance Lanczos, Arnoldi, or Jacobi-Davidson. In such methods the approximations to the wanted eigenvalues and eigenvectors are extracted from projections of the eigenproblem to a series of nested, low dimensional subspaces built in the course of the algorithm.

Let $V \in \mathbb{R}^{n \times k}$ be an (orthonormal) basis of the current search space $\mathcal{V} \subset \mathbb{R}^n$, and assume that $(\theta, y), y \in \mathbb{R}^k$ is an eigenpair of the projected eigenvalue problem

$$V^T S(\lambda) V y = 0,$$

and denote by $x := Vy$ the corresponding Ritz vector. To obtain an improved approximation it is reasonable to expand $\mathcal{V}$ in a direction with a high approximation potential for the eigenvector wanted next.

In the literature one comes across in general two strategies for the subspace expansion: the Jacobi-Davidson type methods like [31] for the polynomial and [8] for the general nonlinear eigenvalue problem, and methods based on the residual inverse iteration, like the nonlinear Arnoldi method [37] for general nonlinear eigenvalue problem or the quadratic Arnoldi method [25, 26] for the special case of the quadratic eigenvalue problem. In this work we restrict ourselves to the latter type of methods, in particular to the nonlinear Arnoldi method as the problems at hand are rational eigenvalue problems. This decision is based on our numerical experience (see Section 3.5 in [4] for a detailed discussion) that for problems with a relatively small number of confined states and of moderate size (allowing for the computation of a good quality preconditioner) the nonlinear Arnoldi method outperforms the Jacobi Davidson type methods.

Residual inverse iteration, introduced by Neumaier [27], suggests the expansion

$$v = S(\sigma)^{-1} S(\theta) x,$$

of the search space $\mathcal{V}$, where σ is a fixed parameter close to the wanted eigenvalues. For a linear eigenproblem $S(\lambda) = A - \lambda B$ this is exactly the Cayley transformation with the pole σ and the zero θ, and since $(A - \sigma B)^{-1}(A - \theta B) = I + (\sigma - \theta)(A - \sigma B)^{-1}B$ and due to shift-invariance of Krylov spaces the resulting projection method is nothing else but a shift-and-invert Arnoldi method.

If the linear system $S(\sigma)v = S(\theta)x$ is too expensive to solve for v, we may choose an approximate solution as a new direction $v = K^{-1}S(\theta)x$ with $K \approx S(\sigma)$. For the linear problem we then obtain an inexact Cayley transformation or a preconditioned Arnoldi method. The resulting iterative projection method given in Algorithm 1, is therefore called nonlinear Arnoldi method, although no Krylov space is constructed and no Arnoldi recursion holds. There are many details that have to be considered when implementing the nonlinear Arnoldi method concerning the choice of the initial basis, when and how to update the preconditioner, and how to restart the method. A detailed discussion is given in [37].

Applying iterative projection method to a general nonlinear eigenvalue problem while approximating more than one eigenpair, it is crucial to prevent the algorithm from converging to the same eigenpair repeatedly, which could adversely affect the convergence speed. For linear eigenvalue problems this is easily achieved by using Schur forms or generalized Schur forms for the projected problem and then locking or purging certain eigenvectors. For nonlinear problems, though, such normal forms do not exist thus presenting a challenge in maintaining good convergence properties.

However, as it can be seen from Theorem 5.1 the eigenvalues of a symmetric nonlinear eigenproblem admitting a minmax characterization can be computed safely one after another. For general nonlinear eigenvalue problems Kressner [17] recently published an approach based on invariant pairs which avoids repeated convergence of eigenpairs,

---

Algorithm 1 Nonlinear Arnoldi Method

1: start with an initial pole σ and an initial orthonormal basis V, $V^*V = I$
2: determine preconditioner $K \approx S(\sigma)$, σ close to the smallest eigenvalue
3: $k = 1$
4: **while** $k \leq$ number of wanted eigenvalues **do**
5:    compute the kth smallest eigenvalue θ and the corresponding normalized eigenvector y of the projected problem $V^T S(\theta) V y = 0$
6:    compute the Ritz vector $u = Vy$ and the residual $r = S(\theta)u$
7:    **if** $\|r\| < \varepsilon$ **then**
8:       accept eigenvalue $\lambda_k = \theta$, and eigenvector $x_k = u$,
9:       choose new pole σ and update preconditioner $K \approx S(\sigma)$ if indicated
10:      restart if necessary
11:      $k = k+1$
12:   **end if**
13:   solve $Kv = r$ for v
14:   $v = v - VV^*v$, $\tilde{v} = v/\|v\|$, $V = [V,\tilde{v}]$
15:   reorthogonalize if necessary
16: **end while**

---

however his approach in its present form seems not suitable for large sparse eigenvalue problems.

Theorem 5.1 provides the connection between the nonlinear eigenvalue problem and the linear eigenvalue problem (5.2) resulting from fixing the eigenvalue parameter λ on the left hand side of (3.2), (4.5), thereby paving the way to exploiting the good numerical properties of linear symmetric eigenvalue problems to target the nonlinear eigenvalue with a specific number. For instance, for the kth eigenpair the minimum in (5.1) is attained for the invariant subspace of $S(\lambda_k)$ corresponding to its k largest eigenvalues, and the maximum by the linear eigenvector of $S(\lambda_k)$ corresponding to the eigenvalue 0.

This very property is at the core of the safeguarded iteration for computing the kth smallest eigenvalue of the projected nonlinear problem $P(\lambda)y := V^T S(\lambda) V y = 0$, in Algorithm 2. The safeguarded iteration has very good convergence properties [28]: It converges globally to the smallest eigenvalue λ_1. The (local) convergence to simple eigenvalues is quadratic. If $P'(\lambda)$ is positive definite, and y in Step 3 of Algorithm 2 is replaced by an eigenvector of $P(\nu_j)y = \mu P'(\nu_j)y$ corresponding to the kth largest eigenvalue, then the convergence is even cubic. Moreover, a variant exists which is globally convergent also for higher eigenvalues, [41].

Algorithm 2 Safeguarded Iteration

1: start with an approximation ν_1 to the kth smallest eigenvalue of $P(\lambda)y = 0$
2: **for** $j = 1,2,\cdots$ until convergence **do**
3:    determine an eigenvector y corresponding to the kth largest eigenvalue of the matrix $P(\nu_j)$
4:    evaluate the Rayleigh functional $\nu_{j+1} = q(y)$, i.e. solve $y^T P(\nu_{j+1})y = 0$ for ν_{j+1}
5: **end for**

---

7   Efficient solution of the pair/quadruple of nonlinear eigenvalue problems

In previous sections, we derived conditions which guarantee that one particular problem of the type (3.2) or (4.5) allows for a minmax characterization of its eigenvalues. If they hold for the problem in question we can apply an iterative projection method like non-linear Arnoldi or Jacobi Davidson and solve each of the problems for $\sigma_z \in \{-1,1\}$ and in the axial symmetric case also for ℓ and $-\ell$ separately. However, as we show now we can do significantly better treating a pair/quadruple of the problems simultaneously, as from our physical intuition we expect the eigensolutions for $\sigma_z = 1$ and $\sigma_z = -1$ and for ℓ and $-\ell$ to be highly related.

We consider two examples: a pyramidal quantum dot and an axially symmetric quantum ring. The matrices for the discretized problem $S_\pm$ were obtained with COMSOL [11] and all the computations were run under MATLAB 7.3 on an Intel Pentium D processor with 4 GByte RAM and 3.2 GHz.

7.1   Pyramidal quantum dot

Our first example is a pyramidal quantum dot (cf. Fig. 1) of height 6.2nm and width 12.4nm embedded into a cuboid matrix $24.8 \times 24.8 \times 18.6[\text{nm}]^3$, which we expose to a ho-mogenous magnetic field of strengths 1,5,10,15,20,25[T] directed along the z-axis.

The pyramid and the matrix are discretized on a tetrahedral grid with quadratic La-grangian elements. The eigenfunctions decay rapidly outside of the dot and the coeffi-cient functions of the differential operator have a jump on the interface. We therefore chose a nonuniform grid, which is fine on the interface between the dot and the matrix (the interface is aligned with the mesh), while coarser in the interior of the dot and the matrix. We limited the maximal size of the elements on the matrix to 10nm, on the dot to 2nm and on the interface to 0.5nm. In this way we obtained a pair of rational matrix eigenvalue problems (5.3) with approximately 46000 degrees of freedom.

Before we apply an iterative projection method, we need to check the conditions (3.5) and (3.7) which guarantee the minmax characterization of the eigenvalues of (3.2). In fact, since we are to apply the method to the discrete problem their discrete counterparts are enough to ensure the convergence of the iterative projection method. The discrete eigenvalue problem corresponding to (3.4) reads

$$Kx = \kappa Mx, \tag{7.1}$$

where K depends on B. The smallest eigenvalue of (7.1) for different values of B are displayed in Table 2. The condition (3.5) holds if

$$\kappa_{min} > \frac{\max\left\{ |\gamma_q^B(\lambda)|, |\gamma_m^B(\lambda)| - V_m \right\}}{\min\left\{ \frac{\hbar^2}{2m_q(\lambda)}, \frac{\hbar^2}{2m_m(\lambda)} \right\}} \quad \forall \lambda \in J, \tag{7.2}$$

Table 2: The smallest eigenvalue of (7.1) for different strengths of magnetic field B.

B [T]	1	5	10	15	20	25
κ_{min}	0.0607	0.0612	0.0629	0.0656	0.0693	0.0739

Table 3: Singular values of $[X_-, X_+]$.

B [T]	σ_1	σ_2	σ_3	σ_4	σ_5
5	1.5085	1.4151	1.4133	1.3132	0.0003
15	1.5096	1.4151	1.4132	1.3119	0.0007
25	1.4194	1.4146	1.4133	1.4095	0.0012

and an elementary discussion of the right hand side demonstrates that (7.2) is even satisfied for $B \leq 500$[T]. Details can be found in the report [6].

Condition (3.7) which secures the existence of the Rayleigh functional is obviously satisfied if

$$\max\left\{\left|\gamma_q^{B'}(\lambda)\right|, \left|\gamma_m^{B'}(\lambda)\right|\right\} \leq 1.$$

Since $\gamma_j^{B'}(\lambda)$ are positive and monotonically falling functions

$$\max_{\lambda \in J}\left\{\left|\gamma_q^{B'}(\lambda)\right|, \left|\gamma_m^{B'}(\lambda)\right|\right\} = \max\left\{\gamma_q^{B'}(0), \gamma_m^{B'}(0)\right\} \approx 0.27 \cdot 10^{-3} B,$$

which remains smaller than 1 for all $B < 3700$[T].

The physical background of the problem, i.e. the splitting of the electronic levels suggests that the eigenfunctions of the pair of problems have some common directions. This conjecture is also supported by the structure of the Zeeman term in (3.2) which involves the sesquilinear form $b_j(\cdot, \cdot)$ and therefore bears some similarity to a "shift".

To verify our guess we compute the cosines of the principal angles spanned by four eigenvectors X_- and X_+ corresponding to the problem S_- and S_+, respectively (i.e. the singular values of $[X_-, X_+]$). The largest singular values are listed in Table 3 for different values of the magnetic field strength B. For all three values of B we observe a clear gap between the 4th and the 5th singular value whereas neither the singular values of X_+ nor those of X_- contain an essential gap. This indicates that the eigensubspaces X_- and X_+ "overlap" substantially. Though this effect wears off with growing B it is still of the order 10^{-3} for a very large $B = 25$[T].

In view of this experiment it appears that solving the pair of problems $S_\pm$ simultaneously allows the solution of one problem to benefit from the solution of the other. This leads to the following approach. We apply an iterative projection method to both problems simultaneously in such a way that they use the same search space $\mathcal{V}$. There are many ways of combining these iterations. We just name the following three:

1. **Fast alternating**: We expand the search space using the residual corresponding to the S_+ and S_-, alternatingly, while iterating the corresponding eigenpairs of S_+ and S_- simultaneously;

2. **Slow alternating**: We alternatingly compute the wanted eigenpairs of S_- and S_+, one by one, while expanding the subspace using the residual of the currently iterated eigenpair;

3. **Sequential**: We first compute all the wanted eigenpairs of S_-, and subsequently the wanted eigenpairs of S_+, while using the residual of the currently iterated eigenpair in the subspace expansion.

The convergence history of these three variants combining two nonlinear Arnoldi iterations for the pair of problems $S_\pm$ and of the single nonlinear Arnoldi iteration for S_- is shown in Fig. 3. The fast alternating method found a pair λ_k^- and λ_k^+ almost immediately after one another, while the slowly alternating version completed the solve for the eigenvalue λ_k^- and then with the acquired knowledge it took only a few iterations for the corresponding eigenvalue λ_k^+. The sequential variant computed all the λ^- first and then the λ^+, gaining less than the other two in terms of the iteration number.

Since the splitting doubles the number of confined states we have to compute, it may be necessary to restart the iteration to keep the time for a solve of the projected problem moderate. We incorporated the restart scheme described in [37] in all variants. We restarted the methods whenever the dimension of the search subspace excluding the eigenvectors exceeded a prescribed threshold and the computation of a pair $\lambda_k^\pm$ was completed. In the sequential variant we also independently restarted, after all λ^- or λ^+, respectively, have been computed. In all cases after restart we kept three more vectors per problem (σ_z, ℓ) than eigenvectors computed so far.

From the convergence plots we learn that the overall number of iterations per four pairs $\lambda_k^\pm$, $k = 1, \cdots, 4$ is comparable for the first two variants, while the third variant needs in either case more iterations. However, in terms of the computation time the third variant, though still slightly slower than the other two if B is small, becomes faster for large values of B. This effect gets more pronounced the more confined states are to be computed. This reflects the fact that if the eigenvectors are strongly related, we loose more throwing away a great part of the already assembled search subspace than when their relation is weaker, in which case we gain more by solving smaller, due to the subspace size reduction, projected problems.

Table 4 displays the CPU times required by the nonlinear Arnoldi method for com-

Table 4: Computation time for the nonlinear Arnoldi method applied to compute 4 smallest eigenvalues of S_- and the second variant of our method applied to the pair $S_\pm$.
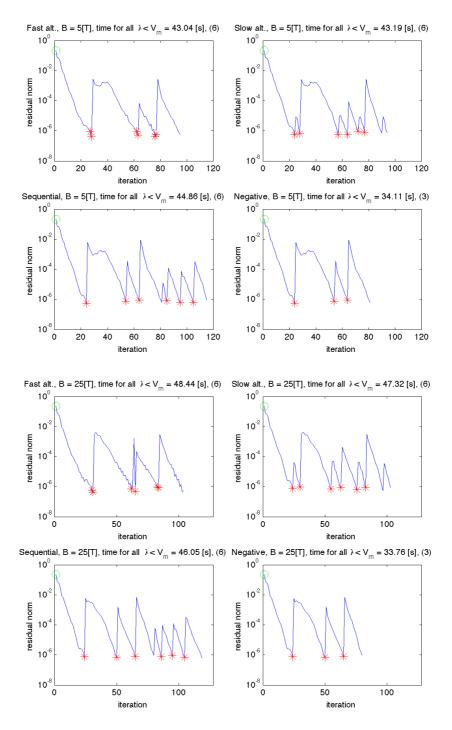
B [T]	total time (N.Arn. S_-) [s]	#iter	total time (2nd v. $S_\pm$) [s]	#iter
1	45.58	80	51.64	86
5	47.22	81	57.32	94
10	47.29	83	61.86	98
15	52.13	88	68.82	104
20	47.96	81	71.14	104
25	45.24	80	72.4	106

Figure 3: Convergence of all three variants of our method for the pair of problems $S_\pm$: subplots 1–3 for $B = 5[T]$ and 5–7 for $B = 25[T]$, and of the nonlinear Arnoldi method for S_-: subplot 4 for $B = 5[T]$ and 8 for $B = 25[T]$. Subplots are numbered left to right and top to bottom.

puting the first four eigenpairs of S_- and by the second variant of our method for the first four pairs $\lambda_k^{\pm}$ of $S_{\pm}$ for different magnetic fields. For all the methods we used the incomplete LU decomposition with the threshold 10^{-2} of $S(0.1)$ (the problem without the magnetic field, $B=0$) as the preconditioner. We did not update the preconditioner during the iteration. The subspace size threshold triggering the restart was set to 200 and was not exceeded by any method, thus except for the third variant no restarts happened.

The deformation and splitting of the energy levels of the pyramidal quantum dot in dependence of the value of the magnetic field strength B is shown in Fig. 5a).

7.2   Quantum ring

Our second example is an elliptical quantum ring obtained by a revolution around the z-axis of an ellipse with the principal axes $a=10$nm (along the r-axis) and $b=2.4$nm (along z-axis), centred at $(r_0,z_0) = (20,0)$nm, embedded in a cylindrical matrix of radius 40nm and height 10nm. As in the previous example we expose the ring to the magnetic field of strengths $B=1,5,10,15,20,25$[T] directed along the z-axis.

We discretized the resulting sequence of two dimensional problems (4.3) on a triangular grid with quadratic Lagrange elements. We aligned the interface with the mesh and limited the maximal element size on the matrix to 4nm, on the dot to 0.5nm, and on the interface to 0.1nm, resulting in approximately 20000 degrees of freedom. To guarantee the convergence of the nonlinear Arnoldi method for the problems (5.4) the discrete versions of conditions (4.7) and (4.8) for all required values of $|\ell|$, here we assume $|\ell|=0,1,2,3$, are checked similarly to the quantum dot case (cf. report [6]).

As in the three dimensional case, we expect the eigenfunctions corresponding to the splitted energy levels to be correlated. However, now we encounter a fourfold if $\ell \neq 0$ and twofold splitting otherwise. This belief can be supported by an experiment similar to Subsection 7.1 (cf. report [6]).

Therefore, it is beneficial to carry out all four iterations simultaneously and let them use the same search subspace. For combining the four iterations we used strategies analogous to those in Section 7.1, with the difference, that we alternated between four problems in first two cases, while in the third variant we compute all the wanted eigenvalues of each of the four problems one after another. The restart strategy was the same as in the previous example. As a preconditioner, we used the incomplete LU with threshold 10^{-2} of S^{ℓ} without the "splitting terms", which was recomputed whenever the convergence rate became to slow.

Fig. 4 shows the convergence of the three variants of our method applied to $S_{\pm}$ for $|\ell|=1$ and of the nonlinear Arnoldi method applied to S_- for $\ell=1$ and $B=5$[T] and $B=25$[T], respectively. Again the most robust variant is the second one, which is the fastest for both the weak and strong magnetic fields. Though, the iteration numbers for the first two variants are comparable the CPU time needed by the first variant is much longer, which is due to the expensive incessant switching between the four problems. Again, we observe that the third variant improves with the growing magnetic field, for
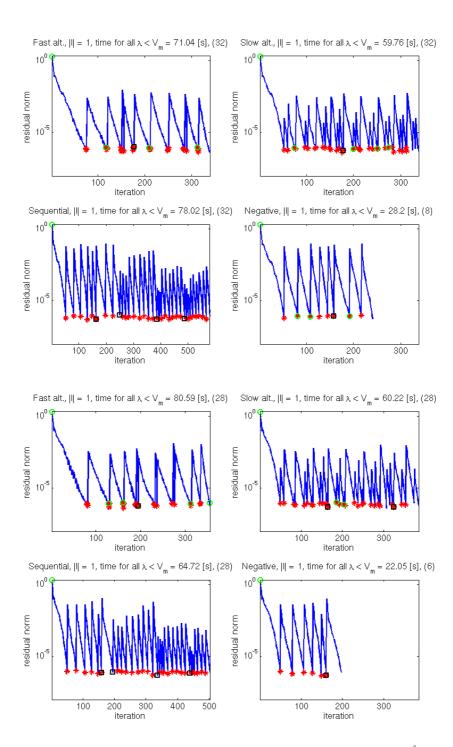
Figure 4: Convergence of all three variants of our method for the quadruple of problems $S_{\pm}^{\ell}$, $|\ell|=1$: subplots 1–3 for $B=5[T]$ and 5–7 for $B=25[T]$, and of the nonlinear Arnoldi method for S_{-}^{ℓ}, $\ell=1$: subplot 4 for $B=5[T]$ and 8 for $B=25[T]$. The squares mark the restarts. Subplots are numbered left to right and top to bottom.
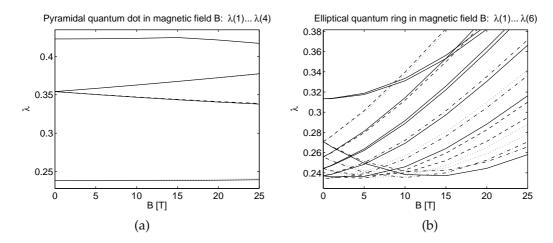
Figure 5: Splitting and deformation of the energy levels of a) pyramidal quantum dot, b) elliptic quantum ring in dependence of the magnetic field B.

the same reason as in our first example. The comparison of the second variant of our method and the nonlinear Arnoldi method in terms of the computation time and the number of iterations is shown in Table 5. For the weak magnetic field, $B = 5[T]$, the gain is about 40% of the CPU time and 65% of the iterations, while for the strong field, $B = 25[T]$, it decreases to 25% and 50%, respectively.

Table 5: Time and iteration number for computation of the confined states by nonlinear Arnoldi applied to S_-^ℓ for $\ell = 1$ and the second variant of our method (Quadruple Simult.N.Arn) applied to $S_\pm^\ell$ for $|\ell| = 1$, for $B = 5,15,25[T]$.

B [T]	N.Arn. CPU [s]	# iter	QS.N.Arn. CPU [s]	# iter
5	32.2	240	76.7	338
15	32.0	240	91.9	362
25	25.4	197	78.0	384

Fig. 5b) shows the splitting and deformation of the first six energy levels (enumeration w.r.t. problem with $B = 0$) in dependence of the magnetic field strength. The effect is much stronger than in the case of the dot, because the ring shape is more prone to trap the perpendicular magnetic field. This results in a periodic oscillations of the electronic levels, see also e.g. [18].

Though in our simulations we have restricted ourselves to the nonlinear Arnoldi method we could as well have used the Jacobi Davison iteration or even combine the two methods. However, our numerical experience is that if the problem size allows for a good quality preconditioner, as it was the case in our examples, the nonlinear Arnoldi method works better. Nevertheless Jacobi Davidson could be the method of choice if the sizes of the eigenvalue problems were much larger.

8   Conclusions

In the framework of one-band nonparabolic effective Hamiltonian in the homogenous magnetic field we derived a pair/quadruple of the nonlinear eigenvalue problems corresponding to different spin orientations and in the case of the rotational symmetry also to $\pm\ell$ quantum number. To the best of our knowledge there is no simulations of truly three dimensional structures like the pyramid in the magnetic field in a nonparabolic regime. We derived conditions for both the three dimensional problem as for the plane problems (resulting from the separation of the axial direction) to allow a minmax characterization of their relevant eigenvalues (confined states). These conditions hold for both our examples of a pyramidal quantum dot and a quantum ring and the common InAs/GaAs heterojunction. In our approach the problems were discretized with Galerkin methods, yielding large and sparse rational matrix eigenvalue problems requiring numerical treatment with iterative projection methods. Endowed with the minmax principle the iterative methods like nonlinear Arnlodi can effectively prevent the repeated convergence to the already computed eigenpairs. For both cases we devised specially tailored iterative methods simultaneously handling the pair/quandruple of the problems and thereby saving about up to 40% of the overall computation time.

Acknowledgments

References

[1] G. Arioli and A. Szulkin. A semilinear Schrödinger equation in the presence of a magnetic field. Arch. Rational Mech. Anal., 170:277–295, 2003.

[2] I. Babuska and J. Osborn. Eigenvalue problems. In P.G. Ciarlet and J.L. Lions, editors, Handbook of Numerical Analysis, volume II, pages 641–923. North Holland, Amsterdam, 1991.

[3] G. Bastard. Wave Mechanics Applied to Semiconductor Heterostructures. Les editions de physique, Les Ulis Cedex, 1988.

[4] M. Betcke. Iterative Projection Methods for Nonlinear Eigenvalue Problems with Applications. Dessertation.de, 2007. PhD Thesis, Hamburg University of Technology.

[5] M. M. Betcke and H. Voss. Stationary Schrödinger equations governing electronic states of quantum dots in the presence of spin-orbit splitting. Applications of Mathematics, 52(3):267–284, 2007.

[6] M. M. Betcke and H. Voss. Efficient solution of stationary Schrödinger equation governing electronic states of quantum dots and rings in magnetic field. Techn. Report 143, Inst. Numer. Simulation, TU Hamburg-Harburg, 2010.

 [7] M. M. Betcke and H. Voss. Numerical simulation of electronic properties of coupled quantum dots on wetting layers. Nanotechnology, 19(16):165204 (10pp), 2008.
 [8] T. Betcke and H. Voss. A Jacobi–Davidson–type projection method for nonlinear eigenvalue problems. Future Generation Computer Systems, 20(3):363–372, 2004.
 [9] S. L. Chuang. Physics of Optoelectronic Devices. John Wiley & Sons, New York, 1995.
[10] M. J. Estaban and P.-L. Lions. Partial Differential Equations and the Calculus of Variations, volume 1, chapter Stationary solutions of nonlinear Schrödinger equations with an external magnetic field. Birkhäuser, Berlin, 1989.
[11] FEMLAB, Version 3.1. COMSOL, Inc., Burlington, MA, USA, 2004.
[12] I. Filikhin, E. Deyneka, G. Melikian, and B. Vlahovic. Electron states of semiconductor quantum ring with geometry and size variations. Molecular Simulation, 31:779–785, 2005.
[13] I. Filikhin, E. Deyneka, and B. Vlahovic. Energy dependent effective mass model of InAs/GaAs quantum ring. Model. Simul. Mater. Sci. Eng., 12:1121–1130, 2004.
[14] C. Hermann and C. Weisbuch. $k \cdot p$ perturbation theory in III-V compounds and alloys: a reexamination. Phys. Rev. B, 15(2):823–833, 1977.
[15] T. M. Hwang, W. W. Lin, W. C. Wang, and W. Wang. Numerical simulation of three dimensional quantum dot. J. Comput. Phys., 196:208–232, 2004.
[16] E. O. Kane. Chapter 3 in Semiconductors and Semimetals, Vol. 1, edited by R. K. Willardson and A. C. Beer, The $k \cdot p$ Method. Academic Press, New York, 1966.
[17] D. Kressner. A block Newton method for nonlinear eigenvalue problems. Numer. Math., 114:355–372, 2009.
[18] B. C. Lee, O. Voskoboynikov, and C. P. Lee. III–IV simiconductor nano-rings. Physica E, 24:87–91, 2004.
[19] Y. Li. Numerical calculation of electronic structure for three-dimensional nanoscale semiconductor quantum dots and rings. J. Comput. Electronics, 2:49–57, 2003.
[20] Y. Li, H.-M. Lu, O. Voskoboynikov, C.P. Lee, and S.M. Sze. Dependence of energy gap on magnetic fields in semiconductor nano-scale quantum rings. Surface Science, 532–535:811–815, 2003.
[21] Y. Li, O. Voskoboynikov, C. P. Lee, S. M. Sze, and O. Tretyak. Effect of shape and size on electron transition energies of InAs semiconductor quantum dots. Jpn.J.Appl.Phys., 41:2698–2700, 2002.
[22] E. H. Lieb and M. Loss. Analysis. Americal Mathematical Society, 2001.
[23] L. C. Lew Yan Voon and M. Willatzen. The $k \cdot p$ Method: Electronic Properties of Semiconductors. Springer-Verlag Berlin Heidelberg, 2009.
[24] M. Markiewicz and H. Voss. Electronic states in three dimensional quantum dot/wetting layer structures. In M. Gavrilova et al. (eds.), editor, Proceedings of ICCSA 2006, volume 3980 of Lecture Notes on Computer Science, pages 684–693, Berlin, 2006. Springer Verlag.
[25] K. Meerbergen. Locking and restarting quadratic eigenvalue solvers. SIAM J. Sci. Comput., 22(5):1814–1839, 2000.
[26] K. Meerbergen. The quadratic Arnoldi method for the solution of the quadratic eigenvalue problem. SIAM Journal on Matrix Analysis and Applications, 30(4):1463–1482, 2008.
[27] A. Neumaier. Residual inverse iteration for the nonlinear eigenvalue problem. SIAM J. Numer. Anal., 22:914–923, 1985.
[28] V. Niendorf and H. Voss. Detecting hyperbolic and definite matrix polynomials. Linear Algebra Appl., 432:1017–1035, 2010.
[29] B. Opic and A. Kufner. Hardy–type inequalities. Longman Scientific & Technical, Essex, England, 1990.

[30] A. A. Sirenko, T. Ruf, N. N. Ledentsov, A. Yu. Egorov, P. S. Kop'ev, V. M. Ustinov, and A. E. Zhukov. Resonant spin-flip Raman scattering and localized exciton luminescence in sub-monolayer InAs-GaAs structures. Solid State Comm., 97, 1996.

[31] G. L. Sleijpen, G. L. Booten, D. R. Fokkema, and H. A. van der Vorst. Jacobi-Davidson type methods for generalized eigenproblems and polynomial eigenproblems. BIT, 36:595 – 633, 1996.

[32] Y. Su and Z. Bai. Solving rational eigenvalue problems via linearization. Techn. Report UC Davis, 2008.

[33] C. G. Van de Walle. Band lineups and deformation potentials in the model-solid theory. Phys. Rev. B 39(3):1871–1883, 1989.

[34] O. Voskoboynikov, Y. Li, H.-M. Lu, C.-F. Shih, and C. P. Lee. Energy states and magnetization in nanoscale quantum rings. Phys. Rev. B, 66:155306–1 – 155306–6, 2002.

[35] O. Voskoboynikov, C. M. J. Wijers, J. L. Liu, and C. P. Lee. Magneto-optical response of layers of semiconductor quantum dots and rings. Phys. Rev. B, 71:245332–1 – 245332–12, 2005.

[36] H. Voss. An Arnoldi method for nonlinear symmetric eigenvalue problems. In Online Proceedings of the SIAM Conference on Applied Linear Algebra, Williamsburg., `http://www.siam.org/meetings/laa03/`, 2003.

[37] H. Voss. An Arnoldi method for nonlinear eigenvalue problems. BIT Numerical Mathematics, 44:387–401, 2004.

[38] H. Voss. A rational eigenvalue problem governing relevant energy states of a quantum dots. J. Comput. Phys., 217:824–833, 2006.

[39] H. Voss. A minmax principle for nonlinear eigenproblems depending continuously on the eigenparameter. Numer. Lin. Algebra Appl., 15:899–913, 2006.

[40] H. Voss and B. Werner. A minimax principle for nonlinear eigenvalue problems with applications to nonoverdamped systems. Math. Meth. Appl. Sci., 4:415–424, 1982.

[41] H. Voss and B. Werner. Solving sparse nonlinear eigenvalue problems. Technical Report Inst. f. Angew. Mathematik, Universität Hamburg, 82/4, 1982.